



Published in final edited form as:

*Chem Biol Drug Des.* 2011 October ; 78(4): 667–678. doi:10.1111/j.1747-0285.2011.01199.x.

## A Disalicylic Acid-Furanyl Derivative Inhibits Ephrin Binding to a Subset of Eph Receptors

Roberta Noberini<sup>‡</sup>, Surya K. De<sup>‡</sup>, Ziming Zhang<sup>‡</sup>, Bainan Wu<sup>‡</sup>, Dhanya Raveendra-Panickar<sup>‡</sup>, Vida Chen<sup>‡</sup>, Jesus Vazquez<sup>‡</sup>, Haina Qin<sup>&</sup>, Jianxing Song<sup>&,#</sup>, Nicholas D. P. Cosford<sup>‡</sup>, Maurizio Pellecchia<sup>‡</sup>, and Elena B. Pasquale<sup>‡,§,\*</sup>

<sup>‡</sup>Sanford-Burnham Medical Research Institute, 10901 North Torrey Pines Road, La Jolla, California 92037

<sup>§</sup>Department of Pathology, University of California, San Diego, California 92093

<sup>&</sup>Department of Biological Sciences, Faculty of Science, National University of Singapore, Singapore 11926

<sup>#</sup>Department of Biochemistry, Yong Loo Lin School of Medicine, National University of Singapore, Singapore 11926

### Abstract

Eph receptor tyrosine kinases and ephrin ligands control many physiological and pathological processes, and molecules interfering with their interaction are useful probes to elucidate their complex biological functions. Moreover, targeting Eph receptors might enable new strategies to inhibit cancer progression and pathological angiogenesis as well as promote nerve regeneration. Because our previous work suggested the importance of the salicylic acid group in antagonistic small molecules targeting Eph receptors, we screened a series of salicylic acid derivatives to identify novel Eph receptor antagonists. This identified a disalicylic acid-furanyl derivative that inhibits ephrin-A5 binding to EphA4 with an IC<sub>50</sub> of 3 μM in ELISA assays. This compound, which appears to bind to the ephrin-binding pocket of EphA4, also targets several other Eph receptors. Furthermore, it inhibits EphA2 and EphA4 tyrosine phosphorylation in cells stimulated with ephrin while not affecting phosphorylation of EphB2, which is not a target receptor. In endothelial cells, the disalicylic acid-furanyl derivative inhibits EphA2 phosphorylation in response to TNFα and capillary-like tube formation on Matrigel, two effects that depend on EphA2 interaction with endogenous ephrin-A1. These findings suggest that salicylic acid derivatives could be used as starting points to design new small molecule antagonists of Eph receptors.

### Keywords

small molecule; antagonist; dymethylpyrrole derivative; protein tyrosine kinase; angiogenesis; nerve regeneration

---

The Eph receptors, which in the human genome comprise fourteen members, represent the largest family of receptor tyrosine kinases. By interacting with their membrane-bound ligands, the ephrins, they regulate a wide range of cellular properties, including cell-substrate and intercellular adhesion, organization of the actin cytoskeleton, and cell shape, movement and growth (1). The Eph receptors are divided into two classes comprising nine

---

\*To whom correspondence should be addressed: Sanford-Burnham Medical Research Institute, 10901 N. Torrey Pines Rd., La Jolla, CA 92037. Phone: (858) 646-3131. Fax: (858) 646-3199. elenap@sanfordburnham.org.

EphA and five EphB receptors according to sequence similarities and binding preferences for the ephrin ligands. The EphA receptors promiscuously bind the five glycosylphosphatidylinositol (GPI)-linked ephrin-A ligands, while the EphB receptors promiscuously bind the three transmembrane ephrin-B ligands, and in addition EphA4 and EphB2 can also bind ephrins of a different class (2). Eph receptor-ephrin binding leads to activation of an intricate network of signaling pathways not only in the Eph receptor-expressing cells (“forward” signaling) but also in the ephrin-expressing cells (“reverse” signaling) (3, 4).

Besides their many roles in normal physiological processes, the Eph receptors have also been linked to various pathological conditions and are therefore considered promising targets for drug development (4–9). In particular, several Eph receptors are highly expressed in different types of cancer, including breast, ovarian, prostate, pancreatic, gastric, lung and brain cancers and melanoma. The roles of Eph receptors in cancer appear to be complex because these receptors can act as either tumor promoters or tumor suppressors, depending on the cell type and the cellular microenvironment. In addition, different Eph receptors may exhibit distinct activities (10, 11).

In tumors where they are activated due to ephrin co-expression, several Eph receptors appear to promote tumorigenicity (12–17). Moreover, the interplay between Eph receptors and ephrins expressed in the tumor vasculature as well as surrounding tumor cells can promote angiogenesis (4). Therefore, interfering with Eph-ephrin binding could be useful for counteracting different aspects of cancer progression. Accordingly, treatment with soluble Eph receptor extracellular domains decreases tumor growth and angiogenesis in various mouse cancer models (18–22). Soluble forms of Eph receptors can also reduce neovascularization in models of retinopathy, another condition where the Eph receptor/ephrin system contributes to blood vessel pathology (23–25). Furthermore, Eph-ephrin interactions can promote platelet aggregation (26), control glucose homeostasis (27) and bone remodeling (28), inhibit nerve regeneration following injury (29), and regulate extracellular glutamate levels in the nervous system (30, 31). Therefore, molecules capable of modulating Eph receptor and ephrin activities could be useful in the treatment of many different pathologies ranging from abnormal blood clotting to diabetes, bone disorders, nervous system injury and neurological diseases characterized by glutamate toxicity. In addition, molecules that selectively target a single Eph receptor or a subset of receptors represent useful tools for investigating the complex functions of Eph receptors in normal physiology and disease.

Besides soluble forms of Eph receptors and ephrins, other molecules that interfere with Eph-ephrin association have been identified, including a number of peptides and three small molecules (32–35). One of these small molecules is a bile acid, lithocholic acid, which was found to similarly inhibit all Eph receptor-ephrin interactions examined (36). The other two small molecules are isomeric salicylic acid-dimethylpyrrole derivatives that we previously identified and found to inhibit ephrin binding to EphA2 and EphA4 (37, 38). In a search for compounds with improved potency and containing chemical entities different from the pyrrole ring, a group that can be problematic (39, 40), we screened a collection of small molecules containing the salicylic acid group. This identified a disalicylic acid-furanyl derivative that inhibits ephrin binding to several Eph receptors as well as Eph receptor activation and biological activities in cultured cells. Further characterization of one of the two salicylic acid-dimethylpyrrole derivatives and the disalicylic acid-furanyl derivative revealed that both compounds may act through non-classical mechanisms of inhibition.

## Methods and Materials

### Chemical synthesis

Compound **3** was synthesized from the starting material **1** with an appropriate boronic acid **2** under Suzuki coupling conditions (Scheme 1). Compound **3** was subjected to microwave irradiation at an output of 350 W for 90 min with acetone in the presence of potassium carbonate at 100°C to generate **4** in moderate yield. Final compound **5** (**76D10**) was obtained by condensation of **4** with compound **3** in the presence of aqueous potassium carbonate in ethanol under microwave irradiation. Compound **76D10** was characterized by NMR and mass spectrometry (MS) and its purity was verified by high-performance liquid chromatography (HPLC) (95% pure) (Supplementary Figure 1; Supplementary Experimental Procedures). The compound was dissolved in DMSO, stored at -20°C and used within 5 weeks. It should be mentioned that one step synthesis of **5** from compound **3** using two equivalents of compound **3** under similar conditions as mentioned above was not successful. Compound **6** (**76B8**) was obtained from compound **3** by hydrolysis in the presence of lithium hydroxide (Scheme 2) while compound **8** (**76A5**) was obtained from compound **3** in the two steps shown in Scheme 2 (see Supplementary Experimental Procedures).

### ELISA assays

Protein A-coated wells (Pierce Biotechnology, Rockford, IL) were used to immobilize Eph receptor Fc fusion proteins (R&D Systems, Minneapolis, MN) incubated at 1 µg/ml in TBST (50 mM Tris-HCl, pH 7.5, 150 mM NaCl, 0.01% Tween 20). Culture supernatants from transfected 293HEK cells and containing ephrin-A5 fused to alkaline phosphatase (ephrin-A5 AP) (32) or ephrin-B2 AP (GeneHunter, Nashville, TN) were diluted in TBST and incubated for 3 hours in the presence or in the absence of compounds, as previously described (37). Alternatively, immobilized ephrin-Fc fusion proteins were incubated with the EphA4 ligand binding domain fused to AP (41). For IC<sub>50</sub> measurements, the AP fusion proteins were used at approximately 0.01 nM (based on AP concentrations calculated from alkaline phosphatase activity (42)). The amount of bound AP-fusion protein was quantified using pNPP as the substrate. Alkaline phosphatase activity from wells with Fc only was subtracted as background. To examine the time dependency of inhibition by **76D10**, the compound was incubated for 30 min to 2 days together with ephrin-A5 AP in wells containing immobilized EphA4 Fc. To determine whether the binding of **76D10** to EphA4 is reversible, the compound was incubated in wells containing immobilized EphA4 Fc for 3 hours and the wells were then washed and incubated in binding buffer for 24 hours to allow dissociation of the compound from EphA4. The wells were then further washed and incubated with ephrin-A5 AP fusion protein for an additional 1 hour. Further control experiments included addition of 0.1 mg/mL bovine serum albumin (BSA, Sigma-Aldrich, Steinheim, Germany) or rat tail collagen (BD Biosciences, San Jose, CA) to the solution containing compound **76D10** and ephrin-A5 AP.

To generate curves for ephrin-A5 AP binding to immobilized EphA4 Fc in the presence of different **76D10** concentrations, data sets at each compound concentration were fitted to the Michaelis-Menten equation:  $B = B_{\max} [S]/(K_D + [S])$ , where [S] is the concentration of ephrin AP fusion protein and  $K_D$  is the dissociation constant, using non linear regression and the program GraphPad (Prism). Ephrin-A5 AP concentrations were calculated from alkaline phosphatase activity (42). Unless otherwise specified, all the binding and washing steps were performed in TBST.

## NMR spectroscopy

The human EphA4 ligand-binding domain (residues 28–208) was prepared as described previously (38). Briefly, the EphA4 cDNA fragment cloned into a modified pET32a vector was transformed into *Escherichia coli* Rosetta (DE3) cells (Novagen). Expression of the EphA4 ligand binding domain with an N-terminal fusion of 16 amino acids containing a hexa-histidine tag (MHHHHHSSGLVPRGS) was induced at 20 °C overnight with 0.4 mM isopropyl 1-thio-D-galactopyranoside. Uniformly  $^{15}\text{N}$ -labeled protein was produced by growing the bacteria in M9 medium with  $^{15}\text{NH}_4\text{Cl}$  as the sole nitrogen source and purified using  $\text{Ni}_2$  affinity chromatography.

NMR spectra were acquired using a 600 MHz Bruker Avance spectrometer equipped with TCI cryoprobe. All NMR data were processed and analyzed using TOPSPIN2.0 (Bruker Biospin Corp., Billerica, MA) and SPARKY (43). 2D- $^{15}\text{N}$ ,  $^1\text{H}$ -HSQC spectra were acquired using 128 scans with 2048 and 128 complex data points in the  $^1\text{H}$  and  $^{15}\text{N}$  dimensions at 300 K. **76D10** binding was detected at 300K by comparing the 2D- $^{15}\text{N}$ ,  $^1\text{H}$ -HSQC spectra of 50  $\mu\text{M}$  EphA4 in the absence and presence of compound at a molar ratio of 6:1. The chemical shift changes were calculated using the following equation (44):

$$(\Delta\text{ppm} = \sqrt{(\Delta^1H)^2 + (0.17 * \Delta^{15}N)^2}).$$

Resonance assignments were obtained by Qin *et al.* (38, 41).

## Measurement of receptor tyrosine phosphorylation in cells

HT22 neuronal cells, which are derived from immortalized mouse hippocampal neurons and endogenously express EphA4 (45), and COS cells (from ATCC), which endogenously express EphA2 and EphB2, were grown in Dulbecco's Modified Eagle's Medium (DMEM) (Mediatech, Inc, Herndon, VA) with 10% fetal bovine serum (FBS) (Hyclone, Logan, UT) and Pen/Strep. PC3 prostate cancer cells, which endogenously express EphA2, were grown in RPMI 1640 medium (Mediatech, Inc, Herndon, VA) with 10% FBS and Pen/Strep. For Eph receptors immunoprecipitations, the cells were serum-starved for 2 hours in serum-free medium and preincubated for 15 min with **76D10** or DMSO as a control. The cells were then stimulated with ephrin-A1 Fc, ephrin-A5 Fc, ephrin-B2 Fc or Fc for 20 min in the continued presence of the compound in serum free-medium. In some experiments, 0.1 mg/mL BSA or collagen were also included in the serum-free medium with **76D10**. To examine the reversibility of **76D10** binding to EphA2 in the cellular context, cells were incubated with the compound for 30 min, washed once in phosphate buffered saline (PBS), and incubated with serum-free medium for 30 min before incubation with ephrin-A1 Fc for 20 min. After stimulation the cells were lysed in modified RIPA buffer (1% Triton X-100, 1% Na deoxycholate; 0.1% SDS; 20 mM Tris; 150 mM NaCl; 1 mM EDTA) containing 10  $\mu\text{M}$  NaF, 1  $\mu\text{M}$  sodium pervanadate and protease inhibitors. Protein concentrations were measured using the BCA protein assay kit (Pierce Biotechnology, Rockford, IL).

For EphA4 immunoprecipitations, HT22 cell lysates were immunoprecipitated with 15  $\mu\text{g}$  anti-EphA4 antibody (46). EphA2 was immunoprecipitated from PC3 cells and COS cells using 2  $\mu\text{g}$  of anti-EphA2 antibody (Millipore-Upstate, Inc, Temecula, CA), while EphB2 was immunoprecipitated from COS cells using 7  $\mu\text{g}$  of an anti-EphB2 antibody made to a glutathione *S*-transferase fusion protein of the EphB2 carboxyl-terminal tail (47). To assess inhibition of EphA2 phosphorylation in response to endothelial cell stimulation with tumor necrosis factor alpha (TNF $\alpha$ ), HUVEC cells (Cascade Biologics, Portland, OG) were grown in Medium 200 supplemented with low serum growth supplements (Cascade Biologics), 10% FBS, Pen/Strep and fungizone. The cells were serum starved for 2 hours in serum-free medium before adding TNF $\alpha$  together with **76D10** or DMSO for 2 hours. Immunoprecipitates and lysates were probed by immunoblotting with anti-phosphotyrosine

antibody (Millipore, Inc, Temecula, CA) and reprobed with antibodies to the respective Eph receptors, followed by a secondary anti-IgG peroxidase-conjugated antibody (GE Healthcare, UK). The EphA2 and EphA4 antibodies used for immunoblotting were from Invitrogen/Zymed Laboratories (San Francisco, CA).

EphA2 phosphorylation was also assessed by ELISA assay. PC3 cells were plated in 24 well plates (Corning, Corning, NY), serum starved in serum-free medium for 1 hour and treated with **76D10** and ephrin-A1 Fc as described above. The cells were then lysed in RIPA buffer or ELISA lysis buffer (20 mM Tris, pH 8.0, 137 mM NaCl, 1% Triton, 10% glycerol, 2 mM EDTA, 1 mM activated Na orthovanadate, 10 µg/ml aprotinin, 10 µg/ml leupeptin). Polystyrene high binding capacity plates (Corning, Corning, NY) were incubated overnight at 4°C with 4 µg/ml goat anti-EphA2 antibody (directed to the extracellular region of the receptor; R&D Systems, Minneapolis, MN) diluted in phosphate buffered saline (PBS), and then incubated for 2 hours at room temperature with cell lysate diluted in RIPA or ELISA lysis buffer. Tyrosine phosphorylation was measured with an anti-phosphotyrosine antibody (Millipore, Inc, Temecula, CA) diluted 1:500, while total EphA2 was measured with a mouse antibody directed to the cytoplasmic region of EphA2 (Invitrogen/Zymed Laboratories, San Francisco, CA) diluted 1:1000 followed by a secondary anti-IgG peroxidase-conjugated antibody (GE Healthcare, UK). 2,2'-azino-bis(3-ethylbenzthiazoline-6-sulfonic acid) (ABTS) (Sigma-Aldrich, Steinheim, Germany) in citric acid was added as a substrate and the absorbance at 405 nm was measured. The absorbance from wells where lysis buffer only was added was subtracted as the background. Unless otherwise specified, all the binding and washing steps were performed in TBST.

### PC3 cell retraction assay

PC3 cells (4,000 cell/well) were plated in 96 well plates (Greiner Bio One, Frickenhausen Germany) and grown for 17 hours. The cells were starved for 1 hour in serum-free RPMI, incubated for 15 min with **76D10** or DMSO, and stimulated for 10 min with 0.5 µg/ml ephrin-A1 Fc or Fc as a control. The cells were then fixed for 15 min in 4% formaldehyde in PBS, permeabilized for 3 min in 0.5% Triton X-100 in TBS, and stained with rhodamine-conjugated phalloidin (Invitrogen). Nuclei were labeled with 4',6-diamidino-2-phenylindole (DAPI). Cells were photographed under a fluorescence microscope and total cell area in the images was measured using Photoshop and ImageJ softwares. Average cell area was calculated dividing total area by the number of cells present measured using ImageJ software.

### MTT assay

The cytotoxicity of **76D10** was measured using the 3-(4,5-dimethylthiazol-2-yl)-2,5-diphenyltetrazolium bromide (MTT) colorimetric assay. Cells were seeded in 96-well plates and treated with compound or DMSO starting 3 or 1 day before they reached 100% confluency. For the assay, MTT (Sigma-Aldrich, St. Louis, MO) was added at a final concentration of 0.5 mg/mL and incubated with the cells for 3 hours. The resulting formazan crystals were then solubilized by addition of 100% DMSO. The absorbance in each well was measured at 570 nm using an ELISA plate reader. The results were expressed as the ratio of the absorbance of cells treated with the compounds or left untreated.

### Tube formation assay

HUVECs ( $2.3 \times 10^4$ ) were grown for 18 hours in 24-well tissue culture plates (Corning, Corning, NY) precoated with 80 µL Matrigel (BD Bioscience, San Jose, CA) in HUVEC complete culture medium containing different concentrations of **76D10**. The length of the tubes and the number of polygons formed were measured from phase contrast images using ImageJ software.

## Results and Discussion

### A disalicylic acid-furanyl derivative inhibits ephrin binding to EphA4 and other Eph receptors

We previously reported the identification of 4- and 5-(2,5 dimethyl-pyrrol-1-yl)-2-hydroxybenzoic acid (compounds **1** and **2**; Table 1) as small molecule antagonists of the EphA2 and EphA4 receptors and highlighted the critical importance of the salicylic acid moiety for the inhibitory activity of the compounds (37, 38). To explore the activity of other small molecules where the salicylic acid group is combined with different chemical entities, we screened a small library of forty-six salicylic acid derivatives (48, 49) for inhibition of ephrin-A5 AP binding to the immobilized EphA4 Fc receptor in ELISA assays (Supplementary Table 1). The two compounds that showed greatest inhibition at 150  $\mu\text{M}$ , **76D10** and **76D6**, were further examined in dose-response curves, which yielded  $\text{IC}_{50}$  values of 4.4  $\mu\text{M}$  and 54  $\mu\text{M}$ , respectively. Thus, the disalicylic acid-furanyl derivative 5,5'-(5,5'-((1E,4E)-3-oxopenta-1,4-diene-1,5-diyl)bis(furan-5,2-diyl))bis(2-hydroxybenzoic acid (**76D10**) is the most active compound of the series, and its average  $\text{IC}_{50}$  value calculated from multiple experiments is  $2.6 \pm 0.4 \mu\text{M}$  (Table 1). Compound **76D10** appears to be somewhat more potent than the previously identified compounds **1** and **2**, which in similar assays inhibited binding with  $\text{IC}_{50}$  values of  $\sim 10 \mu\text{M}$  (37) (but see below). In contrast, two compounds related in structure to **76D10** but containing only one salicylic acid and one furanyl group, (E)-methyl 2-hydroxy-5-(5-(3-methoxy-3-oxoprop-1-en-1-yl)furan-2-yl)benzoate (**76A5**) and 5-(5-formylfuran-2-yl)-2-hydroxybenzoic acid (**76B8**), did not show detectable inhibitory activity in the same assay (Table 1). Thus, the presence of two salicylic acid groups and/or the larger size of compound **76D10** appear to be important for its inhibitory activity.

Binding equilibrium was reached by 3 hours after addition of ephrin-A5 AP with compound **76D10** (Supplementary Figure 2A) and the binding does not appear to be reversible under the conditions used in the ELISA assay (Supplementary Figure 2B). This may be due to the presence of two potential sites for Michael-type reactions in compound **76D10**, which could result in covalent binding to EphA4 or strong non-covalent interactions. The inhibitory activity of **76D10** was lost in the presence of 0.1 mg/ml BSA but was not affected by 0.1 mg/ml collagen (Supplementary Figure 2C), suggesting that the compound binds to BSA but not to proteins in general.

Additional ELISA assays revealed that **76D10** inhibits the binding of EphA4 AP to all ephrin-A and ephrin-B ligands with  $\text{IC}_{50}$  values between 2 and 10  $\mu\text{M}$  (Figure 1A). This is in contrast to compounds **1** and **2**, which do not efficiently inhibit EphA4 AP binding to ephrin-A4 and ephrin-B2 (37). Furthermore, compound **76D10** preferentially inhibits ephrin binding to EphA2 and EphA4 among a number of EphA and EphB receptors examined (Figure 1B), although not as selectively as the previously identified compounds **1** and **2** (37). Indeed, **76D10** also inhibits with substantial potency ephrin-A5 binding to EphA5, EphA6 and EphA7 as well as ephrin-B2 binding to EphB4 and EphB6. However, a much lower to undetectable inhibitory activity of compound **76D10** was observed for inhibition of ephrin binding to EphA3, EphB1, EphB2 and EphB3, ruling out general inhibition of protein-protein interactions and interference with the activity of the alkaline phosphatase reporter.

To more accurately compare the activity of **76D10** and the previously identified compound **1** (Table 1), we decided to measure  $\text{IC}_{50}$  values using freshly synthesized preparations of both compounds because we noticed that **76D10** dissolved in DMSO at concentrations  $\leq 10 \text{ mM}$  becomes less active after several weeks at  $-20^\circ\text{C}$  or several days at room temperature (10 fold increase in  $\text{IC}_{50}$  values after 4 days). Surprisingly, the newly synthesized compound **1** did not show detectable inhibition of ephrin-A5 AP binding to EphA4 Fc in ELISA assays

or EphA2 phosphorylation in cells stimulated with ephrin-A1 Fc (Supplementary Figure 3A,B). However, in the same experiments the purchased compound **1** had an activity comparable to that previously reported (Supplementary Figure 3A,B; (37)), suggesting that an oxidative process gives rise to an active form of compound **1**. Indeed, when left exposed to air at room temperature in dry form, compound **1** acquires a progressively darker brown color. Concomitantly, the compound becomes progressively more active in ELISA assays measuring inhibition of ephrin-A5-EphA4 binding (Supplementary Figure 3A).

Proton and carbon NMR spectra of the active and inactive compound **1** preparations were similar and consistent with the structure of the compound (Supplementary Figure 3C and data not shown). In addition, high-pressure liquid chromatography (HPLC) followed by mass spectrometry (MS) analysis of both the newly synthesized and the purchased compound **1** showed the presence of a major peak whose molecular weight of 232 corresponds to that expected for the compound (Supplementary Figure 3C). These data indicate that while compound **1** in its oxidized form is reproducibly active against the receptor, its inhibitory effect may depend on a redox phenomenon that presumably affects the oxidation state of critical cysteine residues in the receptor rather than a pure antagonism of the ephrin ligands. Nonetheless, to date we have not identified the active component(s) in the preparations of compound **1**, not have definitive experimental proof of the above proposed mechanism. In fact, pyrroles can undergo polymerization, which also results in a dark brown or black color (50). However, this mechanism would not be entirely consistent with the NMR spectra of the compound. These observations are in agreement with the current notion that compounds similar to **1** and **2** are promiscuous in nature and show activity towards a number of other unrelated protein targets (39, 40), perhaps reflecting their ability to undergo different modifications. Nevertheless, it appears that 4-(2,5 dimethylpyrrol-1-yl)-2-hydroxybenzoic acid (i.e. the unmodified compound **1**) has some, albeit weak, ability to bind to EphA4 because  $^1\text{H}$  proton NMR spectra in 10 mM phosphate buffer, pH 6.5, showed resonance peak shifts of compound protons at increasing concentrations of the EphA4 ligand-binding domain (Supplementary Figure 4). In addition, NMR HSQC titrations showed progressively increasing chemical shift perturbations for residues of the EphA4 ligand-binding pocket at increasing concentration of freshly HPLC-purified compound **1** (data not shown), nearly identical to the purchased compound without the additional HPLC purification (38). While the progressive increase in the activity of compound **1** with time following synthesis suggests the occurrence of unknown modifications, compound **76D10** is most active immediately following synthesis. This implies that its active form is that shown in Table 1.

### Compound **76D10** binds to the high affinity ligand-binding pocket of EphA4

The main Eph receptor interface conferring high affinity binding to ephrin ligands is a hydrophobic cavity in the ligand-binding domain that accommodates the G-H loop of the ephrins (51). Although other Eph receptor interfaces participate in ephrin binding, peptides that target the high affinity ligand-binding pocket can inhibit ephrin binding (33, 52, 53). The similar maximal binding ( $B_{\text{max}}$ ) values and increasing dissociation constant ( $K_D$ ) values that were obtained by fitting curves of ephrin-A5 AP binding to EphA4 in the presence of increasing **76D10** concentrations are consistent with competitive inhibition (Figure 1C). However, while its activity does not depend on direct oxidation, compound **76D10** contains a potentially reactive divinylketone group, hence we cannot exclude that this compound also may act in an indirect, non-specific manner. Hence, we carried out two-dimensional NMR  $^1\text{H}$ - $^{15}\text{N}$  HSQC to monitor the binding of the compound. The spectra show that a number of peaks corresponding to residues that line the high affinity ligand-binding pocket of EphA4 undergo significant chemical shift perturbation or disappear in the presence of

**76D10**, consistent with a slow off rate (Figure 2). Taken together, these results strongly suggest that **76D10** targets the high affinity ligand-binding pocket of EphA4.

Interestingly, in all ephrin-A ligands the G-H loop, which mediates the high affinity interaction with EphA receptors, contains the amino acid motif (Y/F)XX(Y/F) – where Y indicates a tyrosine, F a phenylalanine, and X any amino acid (32, 34). This same motif is also found in several peptides that bind to EphA2 and EphA4. The phenyl rings in the salicylic acid groups of **76D10** may recapitulate some of the interactions of the Y/F amino acids with the EphA4 ligand-binding pocket, despite a distinct overall three-dimensional arrangement of **76D10** and the four-amino-acid peptide motif.

### Compound 76D10 inhibits ephrin-induced EphA2 and EphA4 activation in cells

To examine whether **76D10** can inhibit ephrin-induced Eph receptor activation in cells, we used cells endogenously expressing EphA2 and EphA4, which are the two Eph receptors most potently inhibited by the compound (Figure 1B). By probing EphA2 immunoprecipitates with anti-phosphotyrosine antibodies in immunoblotting experiments, we found that **76D10** inhibits tyrosine phosphorylation (activation) of endogenous EphA2 in COS cells and PC3 prostate cancer cells stimulated with ephrin-A1 Fc (Figure 3A and Supplementary Figure 1D). This was confirmed in ELISA assays measuring EphA2 tyrosine phosphorylation (Figure 3B and Supplementary Figure 1E). Compound **76D10** also inhibits EphA4 tyrosine phosphorylation in HT22 neuronal cells stimulated with ephrin-A5 Fc but not EphB2 tyrosine phosphorylation in COS cells stimulated with ephrin-B2 Fc (Figure 3A), consistent with the Eph receptor selectivity determined in ELISA assays (Figure 1B). Interestingly, inhibition of ephrin-induced EphA2 phosphorylation in PC3 and COS cells by **76D10** was reversible (Supplementary Figure 2D), suggesting that irreversible binding is not required for Eph receptor inhibition by the compound in the cellular environment. Furthermore, the presence of BSA but not collagen in the culture medium inhibited the activity of compound **76D10** (Supplementary Figure 2E). The reduced activity of **76D10** in the presence of BSA suggests that the compound would not be active *in vivo*, where albumin levels are high.

### Compound 76D10 inhibits EphA2-mediated cell retraction in PC3 cells

PC3 cells undergo a dramatic retraction of the cell periphery and assume a rounded morphology after stimulation with ephrin-A1 Fc to activate EphA2 (37, 54). Compound **76D10** significantly counteracts these effects at concentrations between 25 and 100  $\mu\text{M}$  (Figure 3C, D). Notably, the compound does not affect cell morphology in the absence of ephrin, which is an indication that it is not acutely toxic and does not act on many different targets regulating PC3 cell morphology.

### Compound 76D10 inhibits TNF $\alpha$ -induced EphA2 activation and capillary-like tube formation in HUVE cells

We found that compound **76D10** inhibits EphA2 tyrosine phosphorylation in response to stimulation with the angiogenic factor TNF $\alpha$  (Figure 4A), which is known to rapidly upregulate expression of endogenous ephrin-A1 thus causing EphA2 activation in endothelial cells (37, 55). The compound also inhibits capillary-like tube formation in HUVE cells plated on Matrigel (Figure 4B), which also causes upregulation of the ephrin-A1 ligand (56). These effects are not due to cell toxicity because HUVE cell viability assessed using the MTT assay was not affected by treatment with **76D10** at 200  $\mu\text{M}$  for up to one day and minimally affected after three days (Figure 4C).



## Conclusions and Future Directions

Small molecules that like **76D10** target Eph receptors involved in angiogenesis – such as EphA2, EphA4 and EphB4 – may inhibit pathological forms of angiogenesis as well as vascular mimicry in tumors (5, 57–59). Furthermore, studies using an EphA4-targeting peptide suggest possible applications of EphA4 antagonistic small molecules for promoting nerve regeneration after spinal cord injury (60). The ability of a compound to inhibit multiple Eph receptor-ephrin interactions involved in angiogenesis (61–63) or nervous system regeneration (64) may further enhance efficacy. However, the identification of small molecules that inhibit Eph receptor-ephrin interactions and have good lead-like properties has proven to be challenging, as is often the case when searching for small molecule inhibitors of protein-protein interactions (65, 66). Only few examples of Eph-ephrin inhibitory small molecules have been reported so far in the literature (36, 37, 67). The recently discovered lithocholic acid, which is a reversible competitive antagonist capable of inhibiting ephrin-induced Eph receptor tyrosine phosphorylation in cells, was found to inhibit with similar low potency all Eph receptors examined (36). The two salicylic acid-dimethylpyrrole derivatives that we previously reported (37), and have further characterized here, appear to owe their activity to reaction products that remain to be characterized.

In this study, we have identified **76D10** as a disalicylic acid-furanyl derivative that targets a subset of Eph receptors and inhibits the functional effects of EphA2 and EphA4 in cultured cells. **76D10** is the most potent Eph receptor antagonistic small molecule reported so far, which may be partially due to the irreversible nature of its interaction with Eph receptors observed under certain experimental conditions. Although both **76D10** and the active compound **1** derivative appear to function through inhibitory mechanisms that are not typically considered suitable for lead optimization (39, 40), these compounds could nevertheless represent useful tools to gain insight into the functions of Eph receptors. In addition, given the many examples of small molecule drugs that operate by non-classical covalent and/or redox mechanisms combined with specific targeting (68–71), it cannot be excluded that optimization of **76D10** may yield improved compounds to inhibit Eph receptor activation by ephrins. It also cannot be excluded that identification of the active compound **1** derivative and elucidation of its mechanism of action may yield a useful starting point for the design of improved small molecules targeting Eph receptors. Finally, the presence of the salicylic acid group in different classes of small molecules able to interfere with Eph-ephrin interaction suggests that screening additional compounds containing one or multiple salicylic acid groups may also represent a viable strategy for the identification of new Eph receptors antagonists.

## Supplementary Material

Refer to Web version on PubMed Central for supplementary material.

## Acknowledgments

The authors thank John Flanagan for the gift of the AP vector and cells secreting the mouse EphA4 extracellular domain AP fusion protein, and Massimiliano Tognolini and Longqin Hu for helpful discussions. This work was supported by National Institutes of Health grants CA138390 (to EBP and MP) and NS067502 (to EBP and NDPC).

## ABBREVIATIONS

<b>AP</b>	alkaline phosphatase
<b>BSA</b>	bovine serum albumin

<b>ELISA</b>	enzyme-linked immunosorbent assay
<b>GPI</b>	glycosylphosphatidylinositol
<b>HPLC</b>	high-performance liquid chromatography
<b>MS</b>	mass spectrometry
<b>NMR</b>	nuclear magnetic resonance

## References

1. Pasquale EB. Eph receptor signalling casts a wide net on cell behaviour. *Nat Rev Mol Cell Biol.* 2005; 6:462–75. [PubMed: 15928710]
2. Pasquale EB. Eph-ephrin promiscuity is now crystal clear. *Nat Neurosci.* 2004; 7:417–8.
3. Jorgensen C, Sherman A, Chen GI, Pasculescu A, Poliakov A, Hsiung M, et al. Cell-specific information processing in segregating populations of Eph receptor ephrin-expressing cells. *Science.* 2009; 326:1502–9.
4. Pasquale EB. Eph receptors and ephrins in cancer: bidirectional signalling and beyond. *Nat Rev Cancer.* 2010; 10:165–80.
5. Ireton RC, Chen J. EphA2 receptor tyrosine kinase as a promising target for cancer therapeutics. *Curr Cancer Drug Targets.* 2005; 5:149–57.
6. Landen CN, Kinch MS, Sood AK. EphA2 as a target for ovarian cancer therapy. *Expert Opin Ther Targets.* 2005; 9:1179–87.
7. Tandon M, Vemula SV, Mittal SK. Emerging strategies for EphA2 receptor targeting for cancer therapeutics. *Expert Opin Ther Targets.* 2011; 15:31–51.
8. Wykosky J, Debinski W. The EphA2 receptor and ephrinA1 ligand in solid tumors: function and therapeutic targeting. *Mol Cancer Res.* 2008; 6:1795–806.
9. Pasquale EB. Eph-ephrin bidirectional signaling in physiology and disease. *Cell.* 2008; 133:38–52.
10. Kumar SR, Schemet JS, Ley EJ, Singh J, Krasnoperov V, Liu R, et al. Preferential induction of EphB4 over EphB2 and its implication in colorectal cancer progression. *Cancer Res.* 2009; 69:3736–45.
11. Astin JW, Batson J, Kadir S, Charlet J, Persad RA, Gillatt D, et al. Competition amongst Eph receptors regulates contact inhibition of locomotion and invasiveness in prostate cancer cells. *Nat Cell Biol.* 2010; 12:1194–204.
12. Hess AR, Seftor EA, Gardner LM, Carles-Kinch K, Schneider GB, Seftor RE, et al. Molecular regulation of tumor cell vasculogenic mimicry by tyrosine phosphorylation: role of epithelial cell kinase (Eck/EphA2). *Cancer Research.* 2001; 61:3250–5.
13. Nakada M, Niska JA, Miyamori H, McDonough WS, Wu J, Sato H, et al. The phosphorylation of EphB2 receptor regulates migration and invasion of human glioma cells. *Cancer Res.* 2004; 64:3179–85.
14. Nakada M, Niska JA, Tran NL, McDonough WS, Berens ME. EphB2/R-Ras signaling regulates glioma cell adhesion, growth, and invasion. *Am J Pathol.* 2005; 167:565–76.
15. Yang NY, Pasquale EB, Owen LB, Ethell IM. The EphB4 Receptor-tyrosine Kinase Promotes the Migration of Melanoma Cells through Rho-mediated Actin Cytoskeleton Reorganization. *J Biol Chem.* 2006; 281:32574–86.
16. Margaryan NV, Strizzi L, Abbott DE, Seftor EA, Rao MS, Hendrix MJ, et al. EphA2 as a promoter of melanoma tumorigenicity. *Cancer Biol Ther.* 2009; 8
17. Yang NY, Lopez-Bergami P, Goydos JS, Yip D, Walker AM, Pasquale EB, et al. The EphB4 receptor promotes the growth of melanoma cells expressing the ephrin-B2 ligand. *Pigment Cell Melanoma Res.* 2010; 23:684–7.
18. Brantley DM, Cheng N, Thompson EJ, Lin Q, Brekken RA, Thorpe PE, et al. Soluble Eph A receptors inhibit tumor angiogenesis and progression in vivo. *Oncogene.* 2002; 21:7011–26.

19. Cheng N, Brantley D, Fang WB, Liu H, Fanslow W, Cerretti DP, et al. Inhibition of VEGF-dependent multistage carcinogenesis by soluble EphA receptors. *Neoplasia*. 2003; 5:445–56.
20. Dobrzanski P, Hunter K, Jones-Bolin S, Chang H, Robinson C, Pritchard S, et al. Antiangiogenic and antitumor efficacy of EphA2 receptor antagonist. *Cancer Res*. 2004; 64:910–9.
21. Martiny-Baron G, Korff T, Schaffner F, Esser N, Eggstein S, Marme D, et al. Inhibition of tumor growth and angiogenesis by soluble EphB4. *Neoplasia*. 2004; 6:248–57.
22. Kertesz N, Krasnoperov V, Reddy R, Leshanski L, Kumar SR, Zozulya S, et al. The soluble extracellular domain of EphB4 (sEphB4) antagonizes EphB4-EphrinB2 interaction, modulates angiogenesis, and inhibits tumor growth. *Blood*. 2006; 107:2330–8.
23. Chen J, Hicks D, Brantley-Sieders D, Cheng N, McCollum GW, Qi-Werdich X, et al. Inhibition of retinal neovascularization by soluble EphA2 receptor. *Exp Eye Res*. 2006; 82:664–73.
24. Zamora DO, Davies MH, Planck SR, Rosenbaum JT, Powers MR. Soluble forms of EphrinB2 and EphB4 reduce retinal neovascularization in a model of proliferative retinopathy. *Invest Ophthalmol Vis Sci*. 2005; 46:2175–82.
25. Ehlken C, Martin G, Lange C, Gogaki EG, Fiedler U, Schaffner F, et al. Therapeutic interference with EphrinB2 signalling inhibits oxygen-induced angioproliferative retinopathy. *Acta Ophthalmol*. 2011; 89:82–90.
26. Prevost N, Woulfe DS, Jiang H, Stalker TJ, Marchese P, Ruggeri ZM, et al. Eph kinases and ephrins support thrombus growth and stability by regulating integrin outside-in signaling in platelets. *Proc Natl Acad Sci U S A*. 2005; 102:9820–5.
27. Konstantinova I, Nikolova G, Ohara-Imaizumi M, Meda P, Kucera T, Zarbalis K, et al. EphA-Ephrin-A-mediated beta cell communication regulates insulin secretion from pancreatic islets. *Cell*. 2007; 129:359–70.
28. Edwards CM, Mundy GR. Eph receptors and ephrin signaling pathways: a role in bone homeostasis. *Int J Med Sci*. 2008; 5:263–72.
29. Du J, Fu C, Sretavan DW. Eph/ephrin signaling as a potential therapeutic target after central nervous system injury. *Curr Pharm Des*. 2007; 13:2507–18.
30. Carmona MA, Murai KK, Wang L, Roberts AJ, Pasquale EB. Glial ephrin-A3 regulates hippocampal dendritic spine morphology and glutamate transport. *Proc Natl Acad Sci U S A*. 2009; 106:12524–9.
31. Filosa A, Paixao S, Honsek SD, Carmona MA, Becker L, Feddersen B, et al. Neuron-glia communication via EphA4/ephrin-A3 modulates LTP through glial glutamate transport. *Nat Neurosci*. 2009; 12:1285–92.
32. Koolpe M, Dail M, Pasquale EB. An ephrin mimetic peptide that selectively targets the EphA2 receptor. *J Biol Chem*. 2002; 277:46974–9.
33. Koolpe M, Burgess R, Dail M, Pasquale EB. EphB receptor-binding peptides identified by phage display enable design of an antagonist with ephrin-like affinity. *J Biol Chem*. 2005; 280:17301–11.
34. Murai KK, Nguyen LN, Koolpe M, McLennan R, Krull CE, Pasquale EB. Targeting the EphA4 receptor in the nervous system with biologically active peptides. *Mol Cell Neurosci*. 2003; 24:1000–11.
35. Mitra S, Duggineni S, Koolpe M, Zhu X, Huang Z, Pasquale EB. Structure-activity relationship analysis of peptides targeting the EphA2 receptor. *Biochemistry*. 2010; 49:6687–95.
36. Giorgio C, Hassan Mohamed I, Flammini L, Barocelli E, Incerti M, Lodola A, et al. Lithocholic Acid Is an Eph-ephrin Ligand Interfering with Eph-kinase Activation. *PLoS One*. 2011; 6:e18128. [PubMed: 21479221]
37. Noberini R, Koolpe M, Peddibhotla S, Dahl R, Su Y, Cosford ND, et al. Small Molecules Can Selectively Inhibit Ephrin Binding to the EphA4 and EphA2 Receptors. *J Biol Chem*. 2008; 283:29461–72.
38. Qin H, Shi J, Noberini R, Pasquale EB, Song J. Crystal Structure and NMR Binding Reveal That Two Small Molecule Antagonists Target the High Affinity Ephrin-binding Channel of the EphA4 Receptor. *J Biol Chem*. 2008; 283:29473–84.

39. Baell JB, Holloway GA. New substructure filters for removal of pan assay interference compounds (PAINS) from screening libraries and for their exclusion in bioassays. *J Med Chem*; 2010; 53:2719–40.
40. Sink R, Gobec S, Pecar S, Zega A. False positives in the early stages of drug discovery. *Curr Med Chem*; 2010; 17:4231–55.
41. Qin H, Noberini R, Huan X, Shi J, Pasquale EB, Song J. Structural characterization of the EphA4-Ephrin-B2 complex reveals new features enabling Eph-ephrin binding promiscuity. *J Biol Chem*; 2010; 285:644–54.
42. Flanagan JG, Cheng HJ, Feldheim DA, Hattori M, Lu Q, Vanderhaeghen P. Alkaline phosphatase fusions of ligands or receptors as in situ probes for staining of cells, tissues, and embryos. *Methods in Enzymology*; 2000; 327:19–35.
43. Goddard, TD.; Kneller, DG. SPARKY 3. University of California; San Francisco:
44. Farmer BT 2nd, Constantine KL, Goldfarb V, Friedrichs MS, Wittekind M, Yanchunas J Jr, et al. Localizing the NADP+ binding site on the MurB enzyme by NMR. *Nat Struct Biol*; 1996; 3:995–7.
45. Li Y, Maher P, Schubert D. A role for 12-lipoxygenase in nerve cell death caused by glutathione depletion. *Neuron*; 1997; 19:453–63.
46. Soans C, Holash JA, Pasquale EB. Characterization of the expression of the Cek8 receptor-type tyrosine kinase during development and in tumor cell lines. *Oncogene*; 1994; 9:3353–61.
47. Holash JA, Pasquale EB. Polarized expression of the receptor protein tyrosine kinase Cek5 in the developing avian visual system. *Developmental Biology (Orlando)*; 1995; 172:683–93.
48. Tautz L, Bruckner S, Sareth S, Alonso A, Bogetz J, Bottini N, et al. Inhibition of Yersinia tyrosine phosphatase by furanyl salicylate compounds. *J Biol Chem*; 2005; 280:9400–8.
49. Vazquez J, Tautz L, Ryan JJ, Vuori K, Mustelin T, Pellecchia M. Development of molecular probes for second-site screening and design of protein tyrosine phosphatase inhibitors. *J Med Chem*; 2007; 50:2137–43.
50. Hidalgo FJ, Nogales F, Zamora R. Effect of the pyrrole polymerization mechanism on the antioxidative activity of nonenzymatic browning reactions. *J Agric Food Chem*; 2003; 51:5703–8.
51. Himanen JP, Saha N, Nikolov DB. Cell-cell signaling via Eph receptors and ephrins. *Curr Opin Cell Biol*; 2007; 19:534–42.
52. Chrencik JE, Brooun A, Recht MI, Kraus ML, Koolpe M, Kolatkar AR, et al. Structure and thermodynamic characterization of the EphB4/Ephrin-B2 antagonist peptide complex reveals the determinants for receptor specificity. *Structure*; 2006; 14:321–30.
53. Chrencik JE, Brooun A, Recht MI, Nicola G, Davis LK, Abagyan R, et al. Three-dimensional Structure of the EphB2 Receptor in Complex with an Antagonistic Peptide Reveals a Novel Mode of Inhibition. *J Biol Chem*; 2007; 282:36505–13.
54. Miao H, Burnett E, Kinch M, Simon E, Wang B. Activation of EphA2 kinase suppresses integrin function and causes focal-adhesion-kinase dephosphorylation. *Nat Cell Biol*; 2000; 2:62–9.
55. Pandey A, Shao H, Marks RM, Polverini PJ, Dixit VM. Role of B61, the ligand for the Eck receptor tyrosine kinase, in TNF-alpha-induced angiogenesis. *Science*; 1995; 268:567–9.
56. Sarma V, Wolf FW, Marks RM, Shows TB, Dixit VM. Cloning of a novel tumor necrosis factor-alpha-inducible primary response gene that is differentially expressed in development and capillary tube-like formation in vitro. *Journal of Immunology*; 1992; 148:3302–12.
57. Hess AR, Seftor EA, Gruman LM, Kinch MS, Seftor RE, Hendrix MJ. VE-cadherin regulates EphA2 in aggressive melanoma cells through a novel signaling pathway: implications for vasculogenic mimicry. *Cancer Biol Ther*; 2006; 5:228–33.
58. Wang JY, Sun T, Zhao XL, Zhang SW, Zhang DF, Gu Q, et al. Functional significance of VEGF-a in human ovarian carcinoma: role in vasculogenic mimicry. *Cancer Biol Ther*; 2008; 7:758–66.
59. Xu Y, Zagoura D, Keck C, Pietrowski D. Expression of Eph receptor tyrosine kinases and their ligands in human Granulosa lutein cells and human umbilical vein endothelial cells. *Exp Clin Endocrinol Diabetes*; 2006; 114:590–5.
60. Fabes J, Anderson P, Brennan C, Bolsover S. Regeneration-enhancing effects of EphA4 blocking peptide following corticospinal tract injury in adult rat spinal cord. *Eur J Neurosci*; 2007; 26:2496–505.

61. Yao VJ, Ozawa MG, Trepel M, Arap W, McDonald DM, Pasqualini R. Targeting pancreatic islets with phage display assisted by laser pressure catapult microdissection. *Am J Pathol*; 2005; 166:625–36.
62. Goldshmit Y, Galea MP, Bartlett PF, Turnley AM. EphA4 regulates central nervous system vascular formation. *J Comp Neurol*; 2006; 497:864–75.
63. Kuijper S, Turner CJ, Adams RH. Regulation of angiogenesis by Eph-ephrin interactions. *Trends Cardiovasc Med*; 2007; 17:145–51.
64. Willson CA, Irizarry-Ramirez M, Gaskins HE, Cruz-Orengo L, Figueroa JD, Whittemore SR, et al. Upregulation of EphA receptor expression in the injured adult rat spinal cord. *Cell Transplantation*; 2002; 11:229–39.
65. Wells JA, McClendon CL. Reaching for high-hanging fruit in drug discovery at protein-protein interfaces. *Nature*; 2007; 450:1001–9.
66. Arkin MR, Whitty A. The road less traveled: modulating signal transduction enzymes by inhibiting their protein-protein interactions. *Curr Opin Chem Biol*; 2009; 13:284–90.
67. Tang FY, Chiang EP, Shih CJ. Green tea catechin inhibits ephrin-A1-mediated cell migration and angiogenesis of human umbilical vein endothelial cells. *J Nutr Biochem*; 2007; 18:391–9.
68. Schirmer A, Kennedy J, Murli S, Reid R, Santi DV. Targeted covalent inactivation of protein kinases by resorcylic acid lactone polyketides. *Proc Natl Acad Sci U S A*; 2006; 103:4234–9.
69. Arnold LA, Estebanez-Perpina E, Togashi M, Jouravel N, Shelat A, McReynolds AC, et al. Discovery of small molecule inhibitors of the interaction of the thyroid hormone receptor with transcriptional coregulators. *J Biol Chem*; 2005; 280:43048–55.
70. Dessal AL, Prades R, Giralt E, Smrcka AV. Rational design of a selective covalent modifier of G protein betagamma subunits. *Mol Pharmacol*; 2011; 79:24–33.
71. Singh J, Petter RC, Baillie TA, Whitty A. The resurgence of covalent drugs. *Nat Rev Drug Discov*. 2011; 10:307–17. [PubMed: 21455239]

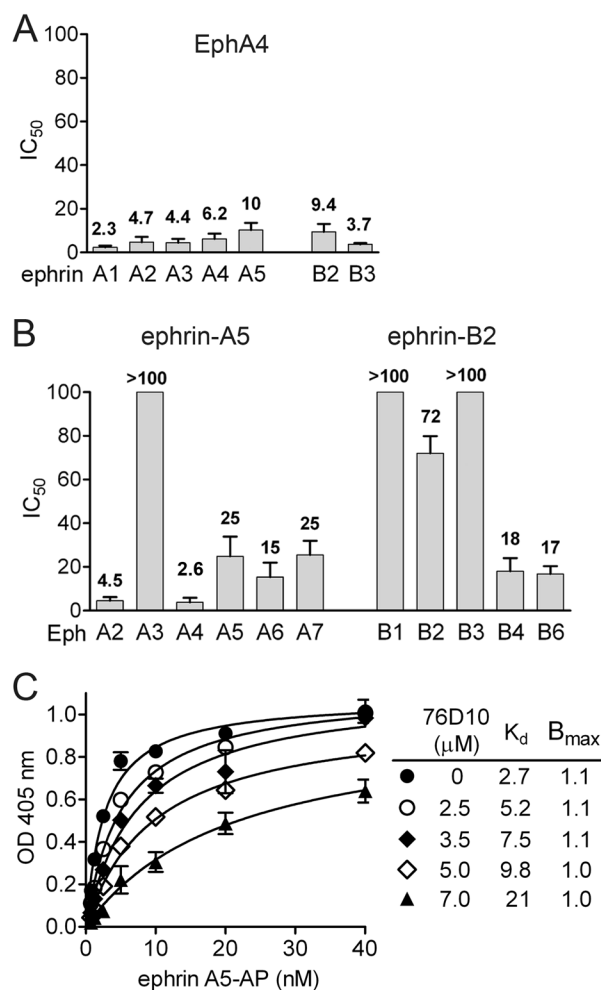


**Figure 1.**

The **76D10** salicylic acid-furanyl derivative inhibits ephrin binding to a subset of Eph receptors. (A) IC<sub>50</sub> values for inhibition of EphA4 AP binding to immobilized ephrin Fc fusion proteins by **76D10**. (B) IC<sub>50</sub> values for inhibition of ephrin-A5 AP binding to immobilized EphA receptor Fc fusion proteins and ephrin-B2 AP binding to immobilized EphB receptor Fc fusion proteins by **76D10**. It should be noted that we typically obtain somewhat lower IC<sub>50</sub> values in this version of the ELISA assay with immobilized Eph receptors compared to the arrangement with immobilized ephrins. Error bars in A and B represent the standard errors for IC<sub>50</sub> values calculated from 3–5 experiments. (C) Curves showing binding of ephrin-A5 AP to immobilized EphA4 Fc in the presence of the indicated concentrations of **76D10**. The curves were fitted according to the Michaelis-Menten equation. Error bars represent the standard errors from triplicate measurements.

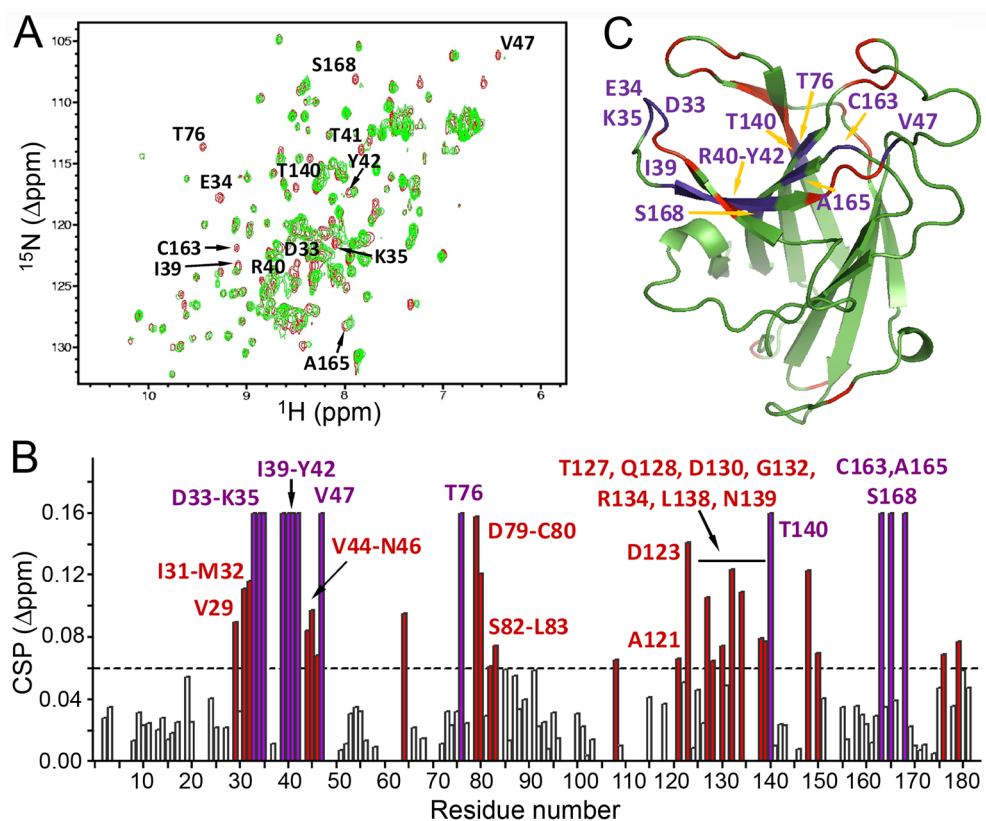


**Figure 2.**

Compound **76D10** causes chemical shifts in residues of the EphA4 ligand-binding pocket. (A) Superposition of  $^1\text{H}$ - $^{15}\text{N}$  NMR HSQC spectra of the EphA4 ligand-binding domain (at a concentration of  $60\ \mu\text{M}$ ) in the absence (red) and in the presence (green) of  $300\ \mu\text{M}$  **76D10**. The residues whose peaks disappeared after the addition of **76D10** are labeled. (B) Residue-specific chemical shift perturbation (CSP) values for the EphA4 ligand-binding domain in the presence of **76D10**. Peaks that disappear from the EphA4 spectrum in panel A are shown as purple bars in the histogram and assigned an arbitrary  $0.16\ \Delta\text{ppm}$  value. A threshold dash line is drawn at  $0.06\ \Delta\text{ppm}$  to indicate residues with significant ( $\Delta\delta > 30\ \text{Hz}$ ) perturbation, which are shown as red bars in the histogram. The amino acids that are part of the EphA4 ligand-binding pocket shown in C are labeled. (C) Ribbon representation of residues in the EphA4 ligand-binding domain that show significant perturbation in the presence of **76D10**. The residues that disappeared from the EphA4 spectrum in A are colored in purple and labeled and the residues with  $\Delta\text{ppm}$  between  $0.06$  and  $0.16$  are shown in red. The structure of the EphA4 ligand-binding domain is from the PDB structure 3CKH, with the missing residues in the loop regions calculated using SWISS-MODEL.

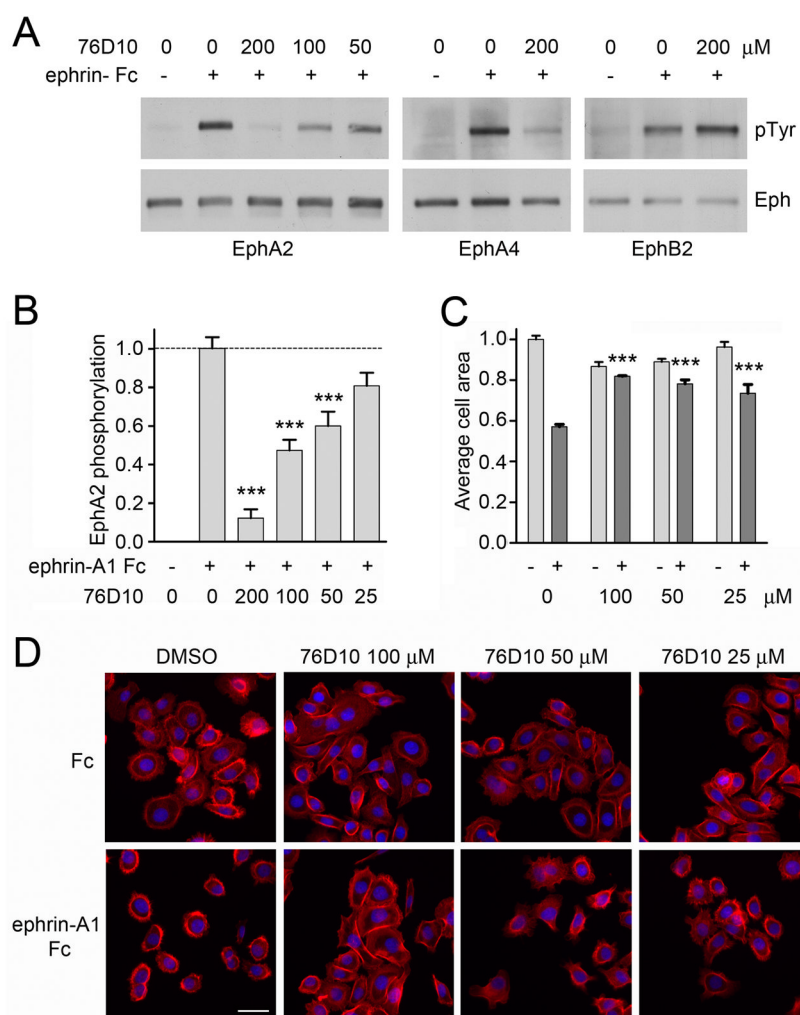


**Figure 3.** Compound **76D10** inhibits EphA4 and EphA2 activation and cell retraction after ephrin stimulation. (A) Cells pretreated with the indicated concentrations of **76D10** for 15 min were stimulated for 20 min with ephrin Fc (+) or Fc (-) as a control in the continued presence of the compound. COS cells were stimulated with 0.2  $\mu\text{g}/\text{mL}$  ephrin-A1 or 0.8  $\mu\text{g}/\text{mL}$  ephrin-B2 Fc and used to immunoprecipitate EphA2 and EphB2, while HT22 neuronal cells were stimulated with 0.2  $\mu\text{g}/\text{mL}$  ephrin-A1 and used to immunoprecipitate EphA4. Eph immunoprecipitates were probed with anti-phosphotyrosine antibody (PTyr) and reprobed for the Eph receptor immunoprecipitated. (B) PC3 cells pretreated for 15 min with the indicated concentrations of **76D10** were stimulated with 0.2  $\mu\text{g}/\text{mL}$  ephrin-A1 Fc (+) or Fc as a control (-) for 20 min in the continued presence of the compound. The histogram shows the average level of phosphorylated EphA2 normalized to the total amount of receptor in the cell lysates, both measured in ELISA assays. Error bars represent standard errors from 4–10 measurements. The levels of EphA2 phosphorylation in cells treated with ephrin-A1 Fc and compound were compared to those in cells treated only with ephrin-A1 Fc by one-way ANOVA and Dunnett's post test. \*\*\* $P < 0.001$  by one-way ANOVA. (C–D) PC3 cells pretreated for 15 min with the indicated concentrations of **76D10** were stimulated with 0.5  $\mu\text{g}/\text{mL}$  ephrin-A1 Fc (+) or Fc as a control (-) for 20 min in the continued presence of the compound. (C) The histogram shows the average area of the cells normalized to the value



obtained for the Fc-treated cells. Error bars represent standard errors from three wells. The average cell areas in cells treated with ephrin-A1 Fc and compound were compared to that in cells treated only with ephrin-A1 Fc by one-way ANOVA and Bonferroni's post test, showing that **76D10** significantly (\*\*P<0.001) inhibits ephrin-A1-dependent cell retraction at concentrations between 100 and 25  $\mu\text{M}$ . The effect of ephrin-A1 was reverted completely by 100  $\mu\text{M}$  76D10 and partially by 50 and 25  $\mu\text{M}$  (comparison between Fc and ephrin-A1 Fc treated samples at each compound concentration yielded P values of >0.05 for 100 $\mu\text{M}$ , <0.05 for 50  $\mu\text{M}$  and <0.001 for 25 $\mu\text{M}$  **76D10**). (D) Representative images of cells stained with rhodamine-phalloidin to label actin filaments (red) and DAPI to label nuclei (blue). Scale bar = 50  $\mu\text{m}$ .

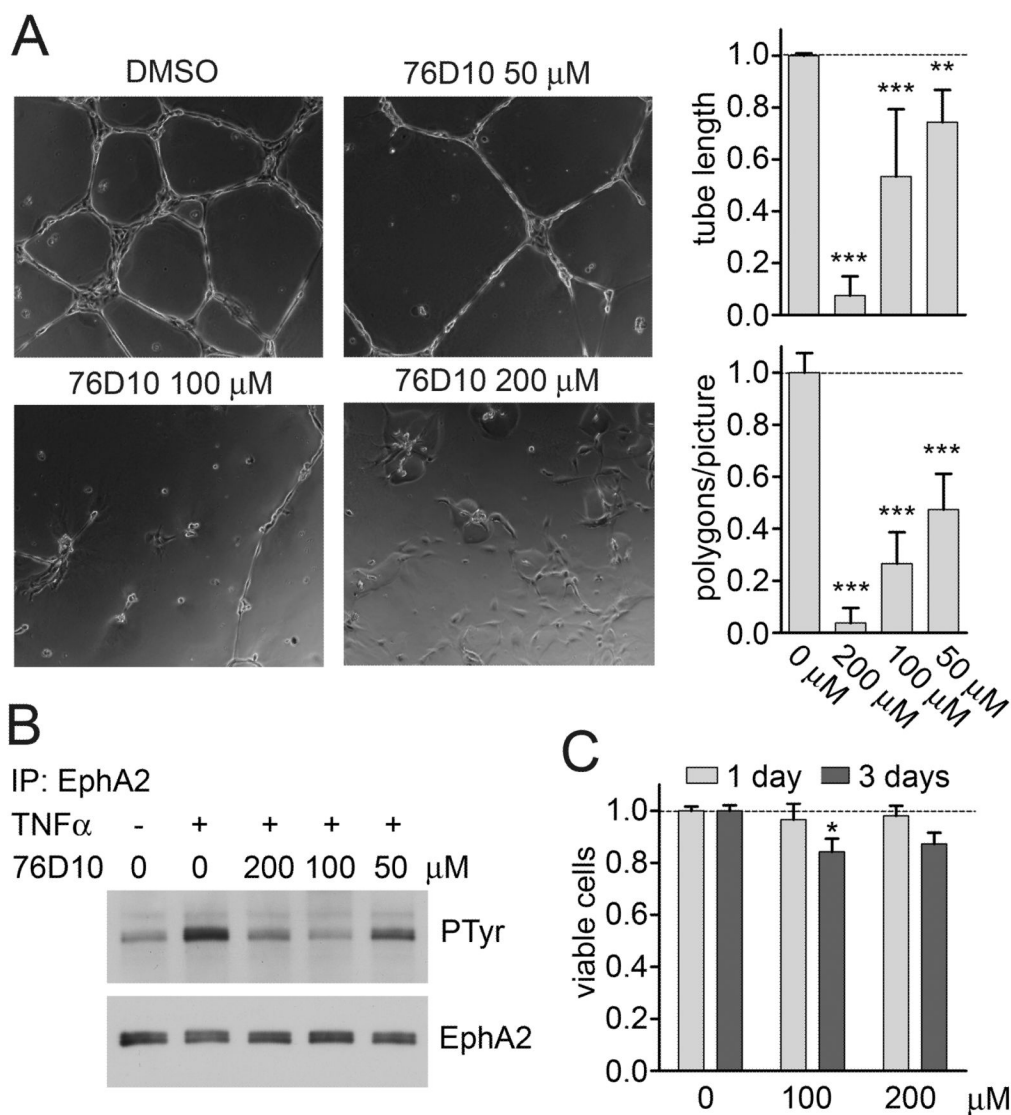
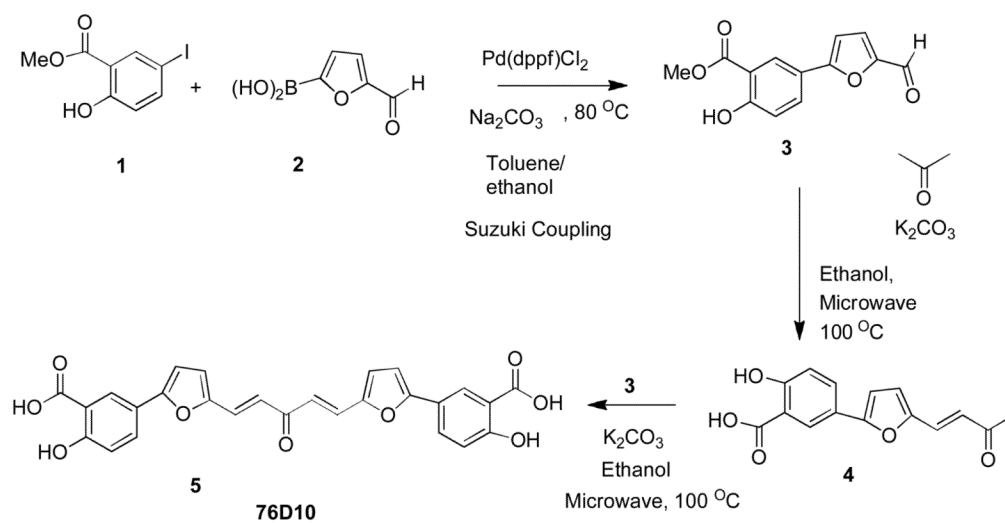
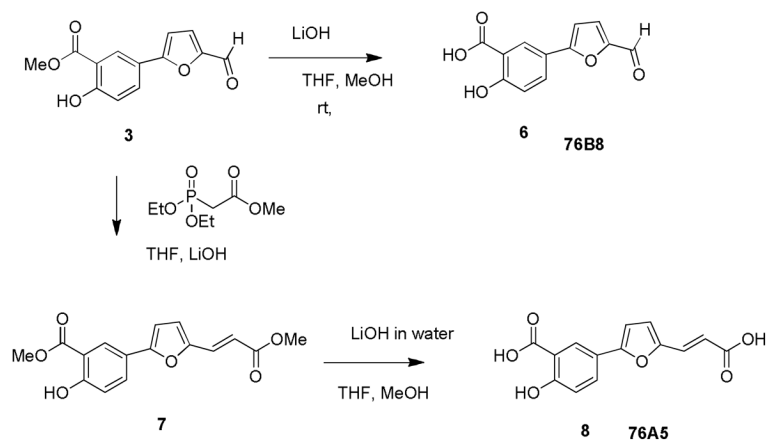


**Figure 4.**

Compound **76D10** inhibits ephrin- and TNF $\alpha$ -induced tyrosine phosphorylation and capillary-like tube formation in HUVE cells. (A) Cells plated on Matrigel were treated with the indicated concentrations of **76D10** or DMSO and imaged 18 hours later. The number of polygons present in each picture and the average tube length were quantified. The histograms show averages from 4 independent experiments and the error bars represent the standard errors. \*\*P<0.01 and \*\*\*P<0.001 by one-way ANOVA and Dunnett's post test. (B) HUVE cells were left unstimulated or stimulated with 20 nM TNF $\alpha$  for 2 hours in the presence of the indicated concentrations of **76D10**. EphA2 immunoprecipitates were probed with anti-phosphotyrosine antibody (PTyr) and reprobed for EphA2. (C) MTT assay to determine the number of viable HUVE cells after growth in the presence of the indicated concentrations of **76D10** for 1 or 3 days. Only DMSO was used in the "0  $\mu$ M" sample, as a control. The histogram shows average absorbance at 570 nm in the presence of **76D10** normalized to the absorbance in the absence of the compound. Error bars represent standard error from 3 measurements in each of two experiments. \*P<0.05 by one-way ANOVA and Dunnett's post test for the comparison to cells not treated with compound (0  $\mu$ M).



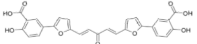
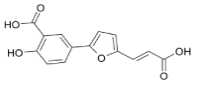
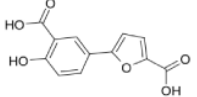
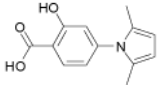
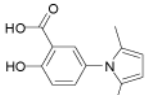
**Scheme 1.**  
Synthesis of 76D10



**Scheme 2.**  
Synthesis of 76A5 and 76B8

**Table 1**

Inhibition of ephrin-A5 AP binding to EphA4 Fc by salicylic acid derivatives

Compound	Structure	MW	IC <sub>50</sub> (μM)
76D10		486	2.6 ± 0.4 (n <sup>**</sup> = 10)
76A5		274	>500 (n = 3)
76B8		232	>500 (n = 3)
Compound 1		232	13 ± 1.3 <sup>**</sup>
Compound 2		232	10 ± 1.6 <sup>**</sup>

\* n, number of experiments;

\*\* from ref. [36].